

Figure 3 Identification of lipoma clarified the reason of intermittent abdominal discomfort in a 29-year-old female. Endoscopic finding (A) and selective small bowel series (B) obtained using double-balloon enteroscopy. This required surgical intervention. An arrow in the B indicates a defect by a lipoma.

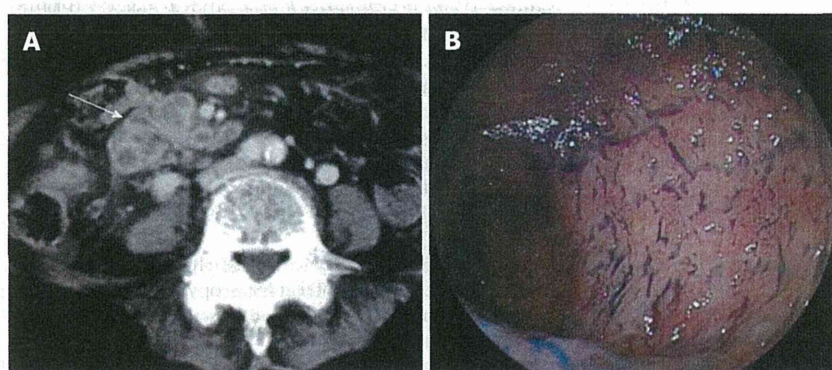


Figure 4 Intestinal tuberculosis is also revealed by double-balloon enteroscopy. A: Computed tomography showed wall thickening of the ileum with contrast enhancement (arrow); B: Double-balloon enteroscopy showed destruction of the small intestinal villi.

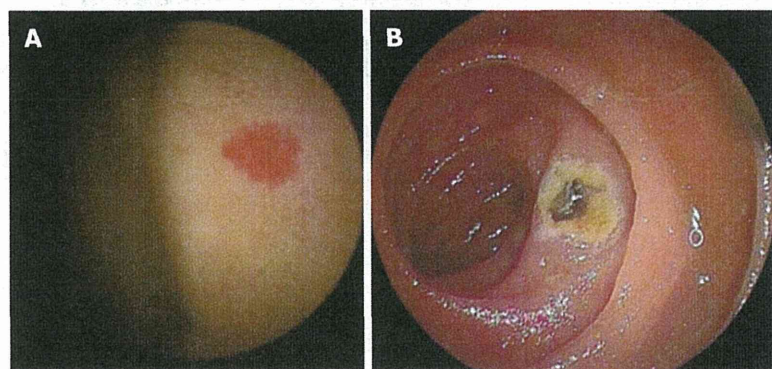


Figure 5 Angioectasia. A: Diagnosis of angioectasia was made by capsule endoscopy; B: Argon plasma coagulation successfully treated the lesion.

above-mentioned authors. The concept of mucosal adaptation^[10] includes proliferation, functional augmentation, and cellular differentiation. Biochemical changes include alterations in molecules related to apoptosis, proliferation, signal transduction, and fatty acid metabolism. These meticulous frameworks in intestinal cells and tissues have so far been revealed by studies using *in vivo* and *in vitro* manipulative systems. From now on, in the era of enteroscopy, lingering questions such as “what is the reality and examples of mucosal adaptation in human clinical settings?” and “how can we validate the accumulated ex-

perimental findings in human beings and exploit them in clinical practice?” will be answered.

Small intestinal enteroscopy is now available in ordinary hospitals, thus facilitating the detection of previously unobserved pathological conditions. Capsular endoscopy, the latest wireless version of enteroscopy, has become a popular practical procedure since the publication of a seminal report on this modality a decade ago^[11]. In the minds of laymen, this technique seems like a dream^[12]. The use of capsular endoscopy and refined enteroscopy using a double-balloon method^[13] in clinical practice have

revealed thousands of new anecdotal findings (Figure 1), and the rapid accumulation of this kind of basic knowledge of the small intestine will help to set up principles of surveillance for mucosal adaptation and atrophy of the small intestine (especially morphological changes) in various clinical conditions. For example, introduction of capsular endoscopy and a double-balloon method disclosed previously unrecognized lesions such as adenocarcinoma arising from Crohn disease in the small intestine (Figure 2)^[14], submucosal lipoma (Figure 3), tuberculosis at the terminal ileum (Figure 4), and angioectasia (Figure 5). None of these lesions were accessible until the recent development of capsule endoscopy and the double balloon method. The morphology is new to pathologists and endoscopists, and these developments will critically influence the managements of the patients. The concepts that Professor Basson and colleagues have illuminated in their review will soon become an important guidepost for evaluating the histopathology of the small intestine in daily practice and for patient care by a broader range of gastroenterologists.

REFERENCES

- 1 Rosai J. Rosai and Ackerman's Surgical Pathology. 9th ed. Edinburgh: Mosby, 2004: 615-872
- 2 Morson BC, Dawson IM, Day DW, Jass JR, Price AB, Williams GT. Morson & Dawson's gastrointestinal pathology. 3 ed. London: Blackwell Scientific Publications, 1989
- 3 Shaw D, Gohil K, Basson MD. Intestinal mucosal atrophy and adaptation. *World J Gastroenterol* 2012; **18**: 6357-6375 [PMID: 23197881 DOI: 10.3748/wjg.v18.i44.6357]
- 4 Tappenden KA. Emerging therapies for intestinal failure. *Arch Surg* 2010; **145**: 528-532 [PMID: 20566971 DOI: 10.1001/archsurg.2010.102]
- 5 Kim JH, Kwon KY, Jeon YK, Nam JH, Choi C, Hyeon CL, Choi YD. Mucin-positive epithelial mesothelioma of the peritoneum: small bowel involvement. *Pathol Int* 2011; **61**: 756-761 [PMID: 22126385 DOI: 10.1111/j.1440-1827.2011.02732.x]
- 6 Kav T, Sivri B. Is enteroscopy necessary for diagnosis of celiac disease? *World J Gastroenterol* 2012; **18**: 4095-4101 [PMID: 22919241 DOI: 10.3748/wjg.v18.i31.4095]
- 7 Oh TG, Chung JW, Kim HM, Han SJ, Lee JS, Park JY, Song SY. Primary intestinal lymphangiectasia diagnosed by capsule endoscopy and double balloon enteroscopy. *World J Gastrointest Endosc* 2011; **3**: 235-240 [PMID: 22110841 DOI: 10.4253/wjge.v3.i11.235]
- 8 Park SC, Chun HJ, Kang CD, Sul D. Prevention and management of non-steroidal anti-inflammatory drugs-induced small intestinal injury. *World J Gastroenterol* 2011; **17**: 4647-4653 [PMID: 22180706 DOI: 10.3748/wjg.v17.i42.4647]
- 9 Tee HP, How SH, Kaffes AJ. Learning curve for double-balloon enteroscopy: Findings from an analysis of 282 procedures. *World J Gastrointest Endosc* 2012; **4**: 368-372 [PMID: 22912911 DOI: 10.4253/wjge.v4.i8.368]
- 10 Drozdowski L, Thomson AB. Intestinal mucosal adaptation. *World J Gastroenterol* 2006; **12**: 4614-4627 [PMID: 16937429]
- 11 Iddan G, Meron G, Glukhovskiy A, Swain P. Wireless capsule endoscopy. *Nature* 2000; **405**: 417 [PMID: 10839527 DOI: 10.1038/35013140]
- 12 Muñoz-Navas M. Capsule endoscopy. *World J Gastroenterol* 2009; **15**: 1584-1586 [PMID: 19340899 DOI: 10.3748/wjg.15.1584]
- 13 Yamamoto H, Sekine Y, Sato Y, Higashizawa T, Miyata T, Iino S, Ido K, Sugano K. Total enteroscopy with a nonsurgical steerable double-balloon method. *Gastrointest Endosc* 2001; **53**: 216-220 [PMID: 11174299]
- 14 Kodaira C, Osawa S, Mochizuki C, Sato Y, Nishino M, Yamada T, Takayanagi Y, Takagaki K, Sugimoto K, Kanaoka S, Furuta T, Ikuma M. A case of small bowel adenocarcinoma in a patient with Crohn's disease detected by PET/CT and double-balloon enteroscopy. *World J Gastroenterol* 2009; **15**: 1774-1778 [PMID: 19360924 DOI: 10.3748/wjg.15.1774]

P- Reviewer Handa O S- Editor Song XX
L- Editor Cant MR E- Editor Zhang DN



Editorial: an obsession with subtyping gastric cancer

Haruhiko Sugimura

Published online: 13 March 2013

© The International Gastric Cancer Association and The Japanese Gastric Cancer Association 2013

Keywords Subtype · Histopathology · Microsatellite instability · Chromosomal numerical abnormality · General rules

My English revisers always correct my ambiguous usage of “type” and “subtype” to describe cancers. I sometimes use “cancer type” in the context of adenocarcinoma versus squamous cell carcinoma, but at other times I use it in the context of gastric cancer versus lung cancer. I am not sure whether to refer to “adenocarcinoma of the lung” as a type or a subtype when discussing a grandiose topic such as the “histopathology of human cancer.”

Categorization was part of human nature even before the work of Carl von Linné, but no categorizations can be more complicated than pathological categorizations, especially those based on the microscopic morphology of cancer cells. Why do we categorize tumors? Lung cancer and gastric cancer are different, so their therapy, care, and prevention measures should also differ. Why must we differentiate between adenocarcinoma and squamous cell carcinoma among cancers arising within the same organ (such as the lung)? Again, therapy (probably), care (possibly), and prevention measures (definitely: for example, avoiding smoking to prevent squamous cell carcinoma of the lung) should be modified according to the tumor category. Then, should we also discriminate among the subtypes of adenocarcinoma of the gastrointestinal tract, such as well-

differentiated versus poorly differentiated? Yes, we know of biological differences between these two subtypes, and a principle of general pathology teaches us that the latter is generally associated with a poorer prognosis. However, we are not sure whether this difference is notable when comparing subtypes at different stages (for example, early-stage poorly differentiated cancer versus advanced-stage well-differentiated cancer). Heterogeneity within a single tumor and heterogeneity among many similar-looking tumors had been known before the era of massive parallel sequencing revolutionized molecular concepts regarding human cancer.

One of my good friends, a confident pulmonary surgeon, once said to me, “No histological description is needed in a breast cancer pathology report; just 3 or 4 immunohistological scores including HER2, hormone receptors, and maybe a proliferation indicator, such as the Ki-67 labeling index.” In the era of companion diagnostics, categorization based on morphology, which is often subjective, may only further complicate clinical cancer management and create an unnecessary burden on pathologists. Actually, every few years the name, subtype categories, and requirements for describing questionable attributes change for unknown reasons and without any emerging evidence but simply because they have been labeled as being a “general rule.” On the other hand, as we approach the brink of personal medicine, the ultimate tumor subtyping—in which the whole genome sequencing of tumor DNA up to the single-cell level will be performed—is appearing on the horizon. The cost of such analyses is becoming less and less and is much less than that of hiring technicians who can make beautifully stained sections. In contrast to morphological classifications, the DNA sequence data can directly pinpoint target molecules that clinicians can then use as a starting point for individualized therapy. Complaints of late

This editorial refers to the article doi:10.1007/s10120-012-0226-6.

H. Sugimura (✉)
Department of Tumor Pathology, Hamamatsu University
School of Medicine, 1-20-1 Handayama, Higashi-ku,
Hamamatsu 431-3192, Japan
e-mail: hsugimur@hama-med.ac.jp

or insufficient pathology reports will disappear, along with the jobs of pathologists. How, then, should the current morphological subtyping be viewed from a molecular perspective?

The first edition of the international histological classification of tumors of the upper gastrointestinal tract, published in 1977, was led and edited by a Japanese pathologist, Dr. Kunio Oota, and pathologists in 13 countries [1]. Dr. Isamu Kino, who was one of the consulting pathologists of that issue, collected and viewed the glass slides of the gastric tumors and then discussed the diagnosis or subtyping with the other participants. The subtypes described for adenocarcinoma continue to be used today [2]: (a) papillary, (b) tubular, (c) mucinous, and (d) signet-ring cell carcinoma. However, the TNM classification prefers a simpler grading: well, moderately, and poorly differentiated [3]. The simplicity of a classification is very important for clinical practice, and the general view of tumors differs according to the stages that are typically encountered by pathologists, which in turn is influenced by the health insurance system, the surveillance system, and the proficiency of diagnostic and screening clinicians in each country. Thus, histological subtypes that can withstand the austerity of medical cost measures must have both a biological and a therapeutic relevance.

In this issue, Tomio Arai, one of the greatest pupils of the late Prof. Kino, has described biological characteristics that are closely related to the morphological subtype. Arai describes a high prevalence of microsatellite instability (MSI) in the papillary subtype of well-differentiated adenocarcinoma and in the solid subtype of poorly differentiated adenocarcinoma of the stomach [4]. Dr. Arai and his colleagues took advantage of a particular series of surgical cases at a single institute, which mainly treats the elderly, and they clearly characterized MSI-positive tumors, which tended to occur in older patients and exhibited a female preponderance and particular histological features. As previously reported, MSI in early-stage adenocarcinoma with papillary features (papillary subtype of well-differentiated adenocarcinoma) is often caused by MLH1 promoter methylation [5], and the concept of field cancerization arising from epigenetic changes has now been extended to and established for other cancers and genes [6]. Arai further showed that a solid subtype of poorly differentiated adenocarcinoma that usually appears as a component in a progressive stage also gains MSI during tumor growth. This finding in solid-subtype tumors implies that the solid subtype, which is usually assigned to a diffuse-type category, should be reassigned as an intestinal type based on the features of its molecular lineage.

Their clear demonstration and meticulous pathological analysis have brought about an end to arguments regarding

MSI and histological features. Earlier reports often concluded that MSI was more prevalent in poorly differentiated, diffuse-type tumors than in intestinal-type tumors [7]. This dichotomy of gastric cancer classification, intestinal versus diffuse type, has often been used by the international community, and the morphological features of the “subtypes” of both categories are often missed. Furthermore, in advanced gastric cancer, the tissues often have a heterogeneous morphology (Prof. Kino often referred to this as a “varied structure”), and they are often MSI positive, which might reflect clonal heterogeneity because the extra bands on the gel are interpreted as evidence of CA repeat slippages [8]. The detailed description of the tissue, including an exact measurement of MSI, is often inadequate, as many laboratory investigators have experienced.

Another issue that Arai addressed is the relationship between MSI and the patient prognosis. Prejudice based on early reports of MSI-positive colon cancer might lead us to expect that MSI-positive tumors are usually associated with a biologically better prognosis [9]. The findings of a better prognosis in MSI-positive cancer cases are probably related to the fact that these MSI-positive cancer cells harbored a near-diploid pattern of DNA. Instead of chromosomal numerical abnormality (CNA), which is related to the extraordinary destruction of genetic material and is strongly correlated with an abysmal prognosis [10], authentic MSI-positive tumors often exhibit a less drastic copy number change in chromosomes [11]. The stage-adjusted analysis performed by Arai et al. did not support a better prognosis for MSI-positive cases in their study. MSI-positive, papillary (sub)type gastric cancer exhibited fewer CNA; thus, CNA information for MSI-positive tumors would be interesting.

The data Arai and his colleagues have provided here will help pathologists to understand the relevance of the subtyping of well-differentiated gastric adenocarcinoma, and this kind of basic support for attributes that many young clinical doctors wrongly believe to be scientifically sound remains scarce in the “general rules” of clinical practice, as most of the required attributes are mainly for research purposes. We should continue to make an effort to validate the significance or insignificance of these attributes so as to edit out the unnecessary ones. Even scientifically sound data, such as those reported by Arai et al., do not necessarily need to be included in conventional pathology reports. Only when these markers are recognized as determinants for the selection of therapeutic measures by several follow-up studies should such obsession with classification become a rule.

Finally, the high autopsy rate at the institution of Arai et al. has provided us with the opportunity to see the natural history and final consequences of cancer in Japanese patients. We congratulate their achievements.

Acknowledgments This contribution was supported, in part, by the Grants-in-Aid for the U.S.–Japan Cooperative Medical Science Program; the National Cancer Center Research and Development Fund; Grant for Priority Areas from the Japanese Ministry of Education, Culture, Sports, Science and Technology (221S0001); and Grants-in-Aid for Cancer Research from the Japanese Ministry of Health, Labour, and Welfare (23120201 and 10103838), and the Princess Takamatsu Cancer Research Fund.

References

1. Oota K, Sobin LH. Histological typing of gastric and oesophageal tumors. Geneva: World Health Organization; 1977.
2. Bosman FT, Carneiro F, Hruban RH, Theise ND. WHO classification of tumours of the digestive system. Lyon: IARC; 2010.
3. TNM classification of malignant tumors. 6th edn. New York: Wiley; 2002.
4. Arai T, Sakurai U, Sawabe M, Honma N, Aida J, Ushio Y, et al. Frequent microsatellite instability in papillary and solid-type, poorly-differentiated adenocarcinomas of the stomach. *Gastric Cancer*. 2013. doi:10.1007/s10120-012-0226-6.
5. Guo RJ, Arai H, Kitayama Y, Igarashi H, Hemmi H, Arai T, et al. Microsatellite instability of papillary subtype of human gastric adenocarcinoma and hMLH1 promoter hypermethylation in the surrounding mucosa. *Pathol Int*. 2001;51(4):240–7.
6. Ushijima T, Hattori N. Molecular pathways: involvement of *Helicobacter pylori*-triggered inflammation in the formation of an epigenetic field defect, and its usefulness as cancer risk and exposure markers. *Clin Cancer Res*. 2012;18(4):923–9.
7. Han HJ, Yanagisawa A, Kato Y, Park JG, Nakamura Y. Genetic instability in pancreatic cancer and poorly differentiated type of gastric cancer. *Cancer Res*. 1993;53(21):5087–9.
8. Wang Y, Shinmura K, Guo RJ, Isogaki J, Wang DY, Kino I, et al. Mutational analyses of multiple target genes in histologically heterogeneous gastric cancer with microsatellite instability. *Jpn J Cancer Res*. 1998;89(12):1284–91.
9. Boland CR, Thibodeau SN, Hamilton SR, Sidransky D, Eshleman JR, Burt RW, et al. A National Cancer Institute Workshop on Microsatellite Instability for cancer detection and familial predisposition: development of international criteria for the determination of microsatellite instability in colorectal cancer. *Cancer Res*. 1998;58(22):5248–57.
10. Suzuki M, Nagura K, Igarashi H, Tao H, Midorikawa Y, Kitayama Y, et al. Copy number estimation algorithms and fluorescence in situ hybridization to describe copy number alterations in human tumors. *Pathol Int*. 2009;59(4):218–28.
11. Song JP, Kitayama Y, Igarashi H, Guo RJ, Wang YJ, Kobayashi T, et al. Centromere numerical abnormality in the papillary, papillotubular type of early gastric cancer, a further characterization of a subset of gastric cancer. *Int J Oncol*. 2002;21(6):1205–11.

Editorial: an obsession with subtyping gastric cancer

Haruhiko Sugimura

Published online: 13 March 2013

© The International Gastric Cancer Association and The Japanese Gastric Cancer Association 2013

Keywords Subtype · Histopathology · Microsatellite instability · Chromosomal numerical abnormality · General rules

My English revisers always correct my ambiguous usage of “type” and “subtype” to describe cancers. I sometimes use “cancer type” in the context of adenocarcinoma versus squamous cell carcinoma, but at other times I use it in the context of gastric cancer versus lung cancer. I am not sure whether to refer to “adenocarcinoma of the lung” as a type or a subtype when discussing a grandiose topic such as the “histopathology of human cancer.”

Categorization was part of human nature even before the work of Carl von Linné, but no categorizations can be more complicated than pathological categorizations, especially those based on the microscopic morphology of cancer cells. Why do we categorize tumors? Lung cancer and gastric cancer are different, so their therapy, care, and prevention measures should also differ. Why must we differentiate between adenocarcinoma and squamous cell carcinoma among cancers arising within the same organ (such as the lung)? Again, therapy (probably), care (possibly), and prevention measures (definitely: for example, avoiding smoking to prevent squamous cell carcinoma of the lung) should be modified according to the tumor category. Then, should we also discriminate among the subtypes of adenocarcinoma of the gastrointestinal tract, such as well-

differentiated versus poorly differentiated? Yes, we know of biological differences between these two subtypes, and a principle of general pathology teaches us that the latter is generally associated with a poorer prognosis. However, we are not sure whether this difference is notable when comparing subtypes at different stages (for example, early-stage poorly differentiated cancer versus advanced-stage well-differentiated cancer). Heterogeneity within a single tumor and heterogeneity among many similar-looking tumors had been known before the era of massive parallel sequencing revolutionized molecular concepts regarding human cancer.

One of my good friends, a confident pulmonary surgeon, once said to me, “No histological description is needed in a breast cancer pathology report; just 3 or 4 immunohistological scores including HER2, hormone receptors, and maybe a proliferation indicator, such as the Ki-67 labeling index.” In the era of companion diagnostics, categorization based on morphology, which is often subjective, may only further complicate clinical cancer management and create an unnecessary burden on pathologists. Actually, every few years the name, subtype categories, and requirements for describing questionable attributes change for unknown reasons and without any emerging evidence but simply because they have been labeled as being a “general rule.” On the other hand, as we approach the brink of personal medicine, the ultimate tumor subtyping—in which the whole genome sequencing of tumor DNA up to the single-cell level will be performed—is appearing on the horizon. The cost of such analyses is becoming less and less and is much less than that of hiring technicians who can make beautifully stained sections. In contrast to morphological classifications, the DNA sequence data can directly pinpoint target molecules that clinicians can then use as a starting point for individualized therapy. Complaints of late

This editorial refers to the article doi:10.1007/s10120-012-0226-6.

H. Sugimura (✉)
Department of Tumor Pathology, Hamamatsu University
School of Medicine, 1-20-1 Handayama, Higashi-ku,
Hamamatsu 431-3192, Japan
e-mail: hsugimur@hama-med.ac.jp

or insufficient pathology reports will disappear, along with the jobs of pathologists. How, then, should the current morphological subtyping be viewed from a molecular perspective?

The first edition of the international histological classification of tumors of the upper gastrointestinal tract, published in 1977, was led and edited by a Japanese pathologist, Dr. Kunio Oota, and pathologists in 13 countries [1]. Dr. Isamu Kino, who was one of the consulting pathologists of that issue, collected and viewed the glass slides of the gastric tumors and then discussed the diagnosis or subtyping with the other participants. The subtypes described for adenocarcinoma continue to be used today [2]: (a) papillary, (b) tubular, (c) mucinous, and (d) signet-ring cell carcinoma. However, the TNM classification prefers a simpler grading: well, moderately, and poorly differentiated [3]. The simplicity of a classification is very important for clinical practice, and the general view of tumors differs according to the stages that are typically encountered by pathologists, which in turn is influenced by the health insurance system, the surveillance system, and the proficiency of diagnostic and screening clinicians in each country. Thus, histological subtypes that can withstand the austerity of medical cost measures must have both a biological and a therapeutic relevance.

In this issue, Tomio Arai, one of the greatest pupils of the late Prof. Kino, has described biological characteristics that are closely related to the morphological subtype. Arai describes a high prevalence of microsatellite instability (MSI) in the papillary subtype of well-differentiated adenocarcinoma and in the solid subtype of poorly differentiated adenocarcinoma of the stomach [4]. Dr. Arai and his colleagues took advantage of a particular series of surgical cases at a single institute, which mainly treats the elderly, and they clearly characterized MSI-positive tumors, which tended to occur in older patients and exhibited a female preponderance and particular histological features. As previously reported, MSI in early-stage adenocarcinoma with papillary features (papillary subtype of well-differentiated adenocarcinoma) is often caused by MLH1 promoter methylation [5], and the concept of field cancerization arising from epigenetic changes has now been extended to and established for other cancers and genes [6]. Arai further showed that a solid subtype of poorly differentiated adenocarcinoma that usually appears as a component in a progressive stage also gains MSI during tumor growth. This finding in solid-subtype tumors implies that the solid subtype, which is usually assigned to a diffuse-type category, should be reassigned as an intestinal type based on the features of its molecular lineage.

Their clear demonstration and meticulous pathological analysis have brought about an end to arguments regarding

MSI and histological features. Earlier reports often concluded that MSI was more prevalent in poorly differentiated, diffuse-type tumors than in intestinal-type tumors [7]. This dichotomy of gastric cancer classification, intestinal versus diffuse type, has often been used by the international community, and the morphological features of the “subtypes” of both categories are often missed. Furthermore, in advanced gastric cancer, the tissues often have a heterogeneous morphology (Prof. Kino often referred to this as a “varied structure”), and they are often MSI positive, which might reflect clonal heterogeneity because the extra bands on the gel are interpreted as evidence of CA repeat slippages [8]. The detailed description of the tissue, including an exact measurement of MSI, is often inadequate, as many laboratory investigators have experienced.

Another issue that Arai addressed is the relationship between MSI and the patient prognosis. Prejudice based on early reports of MSI-positive colon cancer might lead us to expect that MSI-positive tumors are usually associated with a biologically better prognosis [9]. The findings of a better prognosis in MSI-positive cancer cases are probably related to the fact that these MSI-positive cancer cells harbored a near-diploid pattern of DNA. Instead of chromosomal numerical abnormality (CNA), which is related to the extraordinary destruction of genetic material and is strongly correlated with an abysmal prognosis [10], authentic MSI-positive tumors often exhibit a less drastic copy number change in chromosomes [11]. The stage-adjusted analysis performed by Arai et al. did not support a better prognosis for MSI-positive cases in their study. MSI-positive, papillary (sub)type gastric cancer exhibited fewer CNA; thus, CNA information for MSI-positive tumors would be interesting.

The data Arai and his colleagues have provided here will help pathologists to understand the relevance of the subtyping of well-differentiated gastric adenocarcinoma, and this kind of basic support for attributes that many young clinical doctors wrongly believe to be scientifically sound remains scarce in the “general rules” of clinical practice, as most of the required attributes are mainly for research purposes. We should continue to make an effort to validate the significance or insignificance of these attributes so as to edit out the unnecessary ones. Even scientifically sound data, such as those reported by Arai et al., do not necessarily need to be included in conventional pathology reports. Only when these markers are recognized as determinants for the selection of therapeutic measures by several follow-up studies should such obsession with classification become a rule.

Finally, the high autopsy rate at the institution of Arai et al. has provided us with the opportunity to see the natural history and final consequences of cancer in Japanese patients. We congratulate their achievements.

Acknowledgments This contribution was supported, in part, by the Grants-in-Aid for the U.S.–Japan Cooperative Medical Science Program; the National Cancer Center Research and Development Fund; Grant for Priority Areas from the Japanese Ministry of Education, Culture, Sports, Science and Technology (221S0001); and Grants-in-Aid for Cancer Research from the Japanese Ministry of Health, Labour, and Welfare (23120201 and 10103838), and the Princess Takamatsu Cancer Research Fund.

References

1. Oota K, Sobin LH. Histological typing of gastric and oesophageal tumors. Geneva: World Health Organization; 1977.
2. Bosman FT, Carneiro F, Hruban RH, Theise ND. WHO classification of tumours of the digestive system. Lyon: IARC; 2010.
3. TNM classification of malignant tumors. 6th edn. New York: Wiley; 2002.
4. Arai T, Sakurai U, Sawabe M, Honma N, Aida J, Ushio Y, et al. Frequent microsatellite instability in papillary and solid-type, poorly-differentiated adenocarcinomas of the stomach. *Gastric Cancer*. 2013. doi:10.1007/s10120-012-0226-6.
5. Guo RJ, Arai H, Kitayama Y, Igarashi H, Hemmi H, Arai T, et al. Microsatellite instability of papillary subtype of human gastric adenocarcinoma and hMLH1 promoter hypermethylation in the surrounding mucosa. *Pathol Int*. 2001;51(4):240–7.
6. Ushijima T, Hattori N. Molecular pathways: involvement of *Helicobacter pylori*-triggered inflammation in the formation of an epigenetic field defect, and its usefulness as cancer risk and exposure markers. *Clin Cancer Res*. 2012;18(4):923–9.
7. Han HJ, Yanagisawa A, Kato Y, Park JG, Nakamura Y. Genetic instability in pancreatic cancer and poorly differentiated type of gastric cancer. *Cancer Res*. 1993;53(21):5087–9.
8. Wang Y, Shinmura K, Guo RJ, Isogaki J, Wang DY, Kino I, et al. Mutational analyses of multiple target genes in histologically heterogeneous gastric cancer with microsatellite instability. *Jpn J Cancer Res*. 1998;89(12):1284–91.
9. Boland CR, Thibodeau SN, Hamilton SR, Sidransky D, Eshleman JR, Burt RW, et al. A National Cancer Institute Workshop on Microsatellite Instability for cancer detection and familial predisposition: development of international criteria for the determination of microsatellite instability in colorectal cancer. *Cancer Res*. 1998;58(22):5248–57.
10. Suzuki M, Nagura K, Igarashi H, Tao H, Midorikawa Y, Kitayama Y, et al. Copy number estimation algorithms and fluorescence in situ hybridization to describe copy number alterations in human tumors. *Pathol Int*. 2009;59(4):218–28.
11. Song JP, Kitayama Y, Igarashi H, Guo RJ, Wang YJ, Kobayashi T, et al. Centromere numerical abnormality in the papillary, papillotubular type of early gastric cancer, a further characterization of a subset of gastric cancer. *Int J Oncol*. 2002;21(6):1205–11.

Original Article

D2-40-positive lymphatic vessel invasion is not a poor prognostic factor in stage I lung adenocarcinomaKei Shimizu,¹ Kazuhito Funai,¹ Haruhiko Sugimura,² Keigo Sekihara,¹ Akikazu Kawase¹ and Norihiko Shiiya¹¹First Department of Surgery, and ²Department of Tumor Pathology, Hamamatsu University School of Medicine, Hamamatsu, Japan

The present study investigates whether lymphatic vessel invasion (LVI) detected by D2-40 staining is a prognostic factor for stage I adenocarcinoma of the lung. We retrospectively reviewed 124 patients who underwent complete resection for stage I adenocarcinoma of the lung from January 1983 to June 2003. LVI was microscopically evaluated using D2-40 immunostaining. The median follow-up was 71 months. The LVI positive rate was 37%. The 5-year cancer-specific survival rates of the D2-40 positive LVI and negative groups were 88.8% and 84.3%, respectively ($P = 0.630$). The stage I lung adenocarcinoma patients who were determined to be LVI positive based on D2-40 immunostaining did not have a significantly poorer prognosis than the LVI negative cases. Thus, lymphatic microinvasion may not be a prognostic indicator in early lung cancer, although advanced LVI does appear to correlate with survival. It is therefore unnecessary to use D2-40 immunostaining to diagnose LVI in practical settings, and Hematoxylin-Eosin and Elastica van Gieson staining should continue to be used to predict the prognosis of patients with stage I lung adenocarcinoma.

Key words: D2-40 immunostaining, Elastica van Gieson, Hematoxylin-Eosin, lung adenocarcinoma, lymphatic vessel invasion, prognostic factor

Lung cancer is the most common cancer and a major cause of cancer-related death worldwide.¹ The standard treatment of stage I non-small cell lung cancer (NSCLC) is resection. However, even with complete clinical resection, the postoperative survival rate remains unsatisfactory.² Various prog-

nostic factors for lung cancer have been reported;³ lymph node metastasis is known to be a poor prognostic factor for patients with NSCLC.⁴ However, for patients with stage I disease who do not have lymph node metastasis, the prognostic factors are still unclear. Blood vessel invasion (BVI) is considered to be one of the most useful prognostic factors for advanced NSCLC.⁵ However, there are only limited data regarding the relationship between lymphatic vessel invasion (LVI) and the prognosis of stage I NSCLC patients.

Recently, immunostaining with the D2-40 antibody has been reported to be more sensitive for the detection of lymphatic invasion compared with Hematoxylin-Eosin (HE) staining in several types of malignancies, such as uterine cervical, colorectal, breast, and gastric carcinomas.^{6–9} However, there have been only a few reports so far demonstrating a positive correlation between the LVI detected by D2-40-positive vessels and the prognosis.^{10,11} We suggest that the reason that LVI using D2-40 immunostaining has not yet been shown to be a prognostic factor in adenocarcinoma in past reports may be associated with the hypersensitivity in regard to the detection of LVI when D2-40 immunostaining was adopted, namely, D2-40 immunostaining can detect more minute microinvasion. Therefore, we assume that lymphatic microinvasion only detected by D2-40 may not be a prognostic indicator for early lung cancer, and moreover LVI, which is easily detectable by HE and Elastica van Gieson (EVG), has been shown to correlate with the patients survival.

We previously reported lymphatic vessel invasion detected by HE and EVG staining to be a significantly poor prognostic factor for stage IA lung adenocarcinoma.¹² However, the rate of LVI judging using HE and EVG in our previous reported was low, at 62%.¹² In the current study, we re-evaluated these patients with stage I adenocarcinoma of the lung by performing D2-40 immunostaining to the resected blocks in order to detect microinvasive lesions more accurately and to test the hypothesis that D2-40 positive LVI is an independent prognostic factor for stage I lung adenocarcinoma.

Correspondence: Kazuhito Funai, MD, PhD, First Department of Surgery, Hamamatsu University School of Medicine, 1-20-1, Handayama, Higashi-ku, Hamamatsu, Shizuoka 431-3192, Japan. Email: kfunai@hama-med.ac.jp

Conflict of Interest: None declared.

Received 1 November 2012. Accepted for publication 21 March 2013.

© 2013 The Authors

Pathology International © 2013 Japanese Society of Pathology and Wiley Publishing Asia Pty Ltd

PATIENTS AND METHODS

We retrospectively reviewed the records of 124 consecutive patients, admitted from January 1983 to June 2003 with stage I lung adenocarcinoma, who had undergone radical resection at the First Department of Surgery, Hamamatsu University School of Medicine. Patients who received induction chemotherapy or radiotherapy or adjuvant chemotherapy and patients with evidence of a residual tumor at the surgical margin were excluded from this study. All the resected lung cancer cases were assigned to histopathological categories according to the World Health Organization criteria.¹³ For pathological staging, we used the seventh edition of the TNM classification for lung and pleural tumors.⁴ Resected tumors were examined by HE and EVG stain and were sub-typed according to the 2011 International Association for the Study of Lung Cancer, the American Thoracic Society, and the European Respiratory Society (IASLC/ATS/ERS) classification system.¹⁴

Histological evaluation

We newly made adjacent sections from paraffin-embedded blocks, which had been stored at room temperature for more than 8 years in the Diagnostic Pathology Division in Hamamatsu University Hospital at Hamamatsu University School of Medicine. All the sections, cut 3 µm thick, were stained with D2-40, a mouse monoclonal antibody (DAKO, Carpinteria, CA, USA). Immunohistochemical studies of the sections of paraffin-embedded tissues (3 µm) were performed using a Histofine Simple Stain MAX-PO (Nichirei, Tokyo, Japan) for D2-40. Antigen retrieval was performed by heating the sections after immersion in Tris-EDTA buffer (pH 9.0) in a pressure cooker for 30 min.¹⁵ In addition, the sections were incubated with the monoclonal antibody against D2-40 at a concentration of 1:50 (DAKO). LVI was considered to be positive when cancer cells were present, surrounded by lymphoendothelium with D2-40 expression (Fig. 1). All histological sections were reviewed by two physicians (H.S. and K.S.) and evaluated as being either positive or negative LVI by D2-40.

Statistical analysis

The cancer-specific survival was estimated using the Kaplan–Meier method, and any differences in survival were determined by a log-rank analysis. The length of survival was defined as the interval in days between the day of pulmonary resection and date of either death or the last follow-up. An observation was censored at the last follow-up when the patients were alive or had died from a cause other than

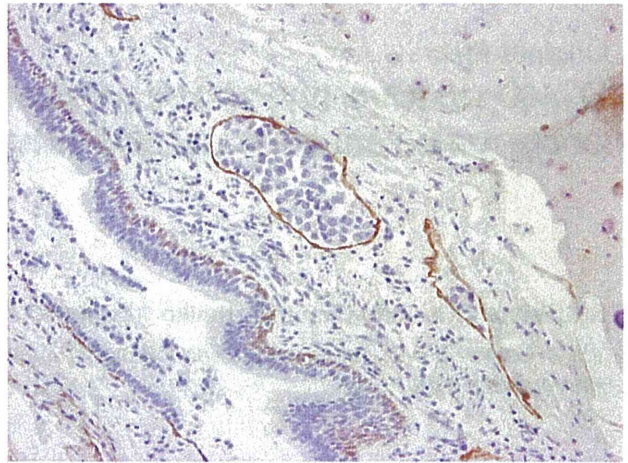


Figure 1 A representative photograph of immunohistochemical staining with D2-40 to evaluate lymphatic invasion (x20).

cancer. All *P*-values were two-sided, and *P*-values ≤ 0.05 were considered to be statistically significant. All statistical analyses were performed with the PASW statistical software package version 18 (SPSS, Inc., Chicago, IL, USA).

RESULTS

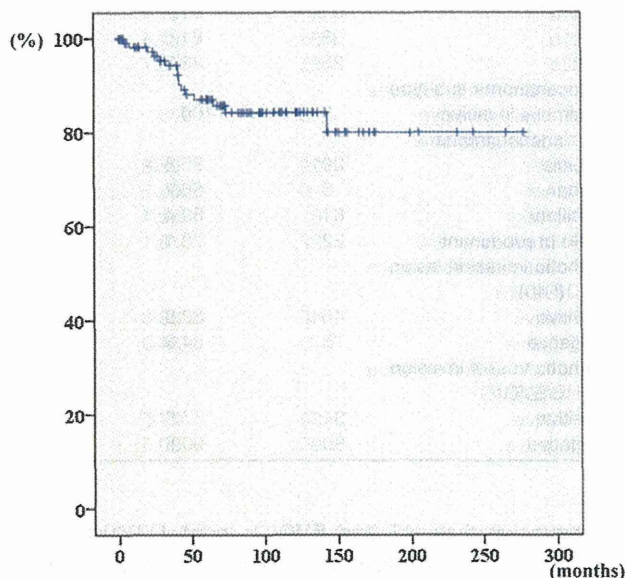
In this study, we reviewed a total of 124 patients who underwent resection of stage I adenocarcinoma of the lung. The patient characteristics are shown in Table 1. This study included 64 males and 60 females, who had a median age of 64 years (range, 38–85 years). In total 66 cases were over 65 years old, 61 cases were pathological stage T1a, 38 cases were pathological T1b, and 25 cases were pathological T2a.

The median follow-up was 71 months. A total of 46 cases (37%) were detected to have LVI with D2-40 immunostaining, and a total of 34 cases (27%) were detected to have LVI with HE and EVG. Table 2 compares the characteristics of patients with and without LVI.

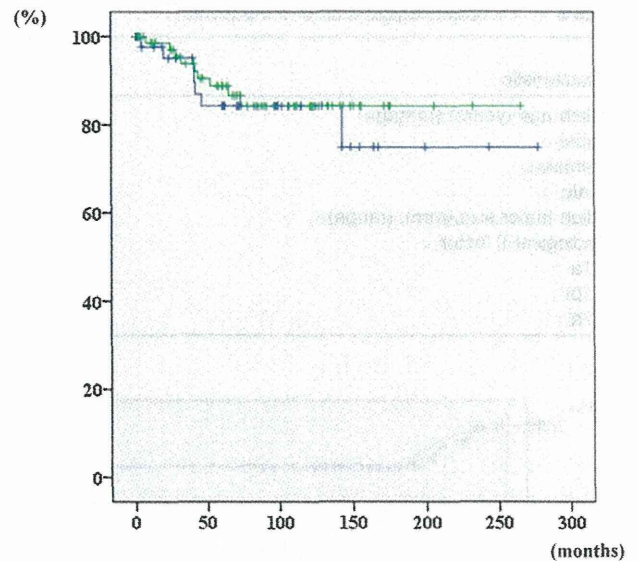
The 5-year survival rate of all patients was 87.1% (Fig. 2). The 5-year survival rates of those over 65 years old and younger than 65 were 85.8% and 88.4%, respectively ($P = 0.791$). The 5-year survival rates of males and females were 80.4% and 93.7%, respectively ($P = 0.225$). The 5-year survival rates of patients with stage T1a, T1b and T2a disease were 91.7%, 81.6% and 83.7%, respectively ($P = 0.080$). The 5-year survival rates of the D2-40 positive LVI and negative LVI were 88.8% and 84.3%, respectively ($P = 0.630$) (Fig. 3). On the other hand, the 5-year survival rates of the LVI-positive group and the LVI-negative group based on HE and EVG staining was 77.5% and 90.5%, respectively ($P = 0.006$) (Fig. 4). About histological sub-typing of adenocarcinoma,

Table 1 Clinicopathological data of 124 patients with stage I lung adenocarcinoma

Characteristic	Number (n = 124)
Median age (years) (range)	64 (38–85)
<65	58
≥65	66
Gender	
Female	60
Male	64
Adenocarcinoma sub-type	
Minimally invasive adenocarcinoma	3
Lepidic	29
Acinar	9
Papillary	61
Solid predominant	22
Pathological T factor	
T1a	61
T1b	38
T2a	25
Lymphatic vessel invasion (D2-40)	
Positive	46 (37%)
Negative	78 (63%)
Lymphatic vessel invasion (HE/EVG)	
Positive	34 (27%)
Negative	90 (73%)

**Figure 2** Overall survival rate of the 124 patients.

three (3%) were minimally invasive adenocarcinoma (MIA) and 121 (97%) were invasive adenocarcinoma, in which 29 (23%) were lepidic (LEP), 9 (7%) were acinar (ACN), 61 (49%) were papillary (PAP), 22 (18%) were solid predominant subtype (SOL). The 5-year cancer-specific survival of patients with MIA were 100%. Those of LEP, ACN, PAP and SOL were 95.8%, 66.7%, 89.4% and 78.1%, respectively ($P = 0.160$).

**Figure 3** The 5-year survival rates of the D2-40 positive LVI and negative LVI was 88.8% and 84.3%, respectively ($P = 0.630$). —, negative; —, positive.

A univariate analysis determined that LVI detected by HE and EVG (positive vs negative: 77.5% vs 90.5%; $P = 0.006$) was a significant prognostic factor (Table 3).

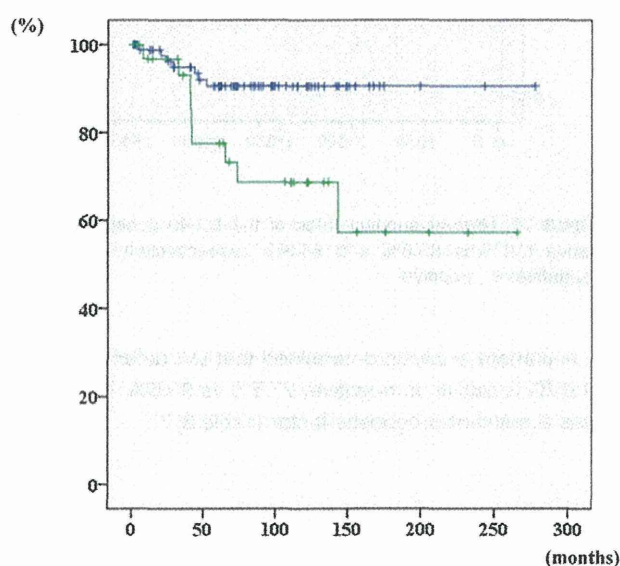
DISCUSSION

Recently, the number of patients with lung cancer has been increasing in Japan. The 5-year overall survival rates of stage IA and IB patients are 73% and 58%, respectively.⁴ The treatment outcome is not satisfactory. It is necessary to identify subjects who are likely to have a poor prognosis among stage I NSCLC patients to recommend that they undergo adjuvant treatment after surgery.

For stage II through IV NSCLC patients, lymph node metastasis is one of the most important prognostic factors. Because stage I NSCLC patients do not have lymph node metastasis, it is necessary to identify other factors. One of the potential prognostic factors is LVI.¹⁶ For detecting LVI, D2-40 immunostaining was reported to be more useful than HE staining.¹⁷ However, there is controversy regarding the impact of D2-40 staining in NSCLC. Some have argued that D2-40-positive LVI is a poor prognostic factor in squamous cell carcinoma of the lung,¹⁸ while others have argued the opposite.¹⁹ In the positive study, the most common histological type was squamous cell carcinoma,¹⁸ and there have been few reports showing a correlation between the LVI determined by D2-40 and prognosis in patients with adenocarcinoma of the lung.^{20,21} We previously reported that the LVI detected by HE and EVG was a significant prognostic

Table 2 Clinicopathological data of the patients

Characteristic	Diagnosis of lymphatic vessel invasion	
	Positive (n = 46)	Negative (n = 78)
Median age (years) (range)	61 (36–83)	65 (33–82)
Gender		
Female	25	36
Male	21	42
Median tumor size (mm), (range)	23 (4–50)	23 (8–50)
Pathological T factor		
T1a	26	34
T1b	12	26
T2a	8	17

**Figure 4** The 5-year survival rates of LVI-positive group and the LVI-negative group based on HE and EVG staining was 77.5% and 90.5%, respectively ($P = 0.006$). □, negative; ■, positive.

factor.¹² Namely, the 5-year overall survival rate of the LVI-negative group and the LVI-positive group was 94.5% and 70.9%, respectively ($P = 0.003$).¹² This previous report focused on the relationship between LVI and the prognosis of stage IA adenocarcinoma based on HE and EVG staining, avoiding the use of the controversial D2-40 immunostaining. In the current study, a similar result was obtained. Namely, LVI detected by HE and EVG (positive vs negative: 77.5% vs 90.5%; $P = 0.006$) was a significant prognostic factor.

In the current study, we examined the correlation between D2-40 positive LVI and the prognosis of stage I lung adenocarcinoma patients who comprised patients that belonged to the same cohort as described in our previous report.¹² The LVI positive rate using D2-40 immunostaining was 37%, and the LVI positive rate using HE and EVG was 27%. Thus indicating that the LVI positive rate was higher in the D2-40 immunostaining group than the HE/EVG staining group. This shows that D2-40 immunostaining can detect more lymphatic

Table 3 The 5-year overall survival rate based on the clinical characteristics

	Number	The 5-year cancer-specific survival	
		rate (%)	<i>P</i> -value
Age			0.791
<65	58	88.4	
≥65	66	85.8	
Gender			0.225
Female	60	93.7	
Male	64	80.4	
Pathological T factor			0.080
T1a	61	91.7	
T1b	38	81.6	
T2a	25	83.7	
Adenocarcinoma sub-type			0.160
Minimally invasive adenocarcinoma	3	100	
Lepidic	29	95.8	
Acinar	9	66.7	
Papillary	61	89.4	
Solid predominant	22	78.1	
Lymphatic vessel invasion (D2-40)			0.630
Positive	46	88.8	
Negative	78	84.3	
Lymphatic vessel invasion (HE/EVG)			0.006
Positive	34	77.5	
Negative	90	90.5	

microinvasion than HE and EVG. In brief, D2-40 immunostaining is more sensitive for detecting LVI than HE and EVG. However, lymphatic microinvasion may not be a prognostic indicator in early lung cancer, although advanced LVI does appear to correlate with survival. In fact, Hashizume *et al.*²¹ reported that there was no significant difference in cancer-specific survival between patients with D2-40-positive LVI and negative groups, while there was a significant difference between patients with low grade invasion group (ly0,1) and those with high grade invasion group (ly2,3) using D2-40 immunostaining. This means that it is not important to distinguish between ly0 and ly1 when looking for a prognostic factor, that is, D2-40 immunostaining can detect more lymphatic microinvasion which may not be a prognostic indicator

in early lung cancer. Therefore, the diagnosis of LVI using HE and EVG staining, which has been performed for a long time, and is affordable for laboratories throughout the world, is better than D2-40 immunostaining for detecting LVI as a prognostic factor for stage I lung adenocarcinoma.

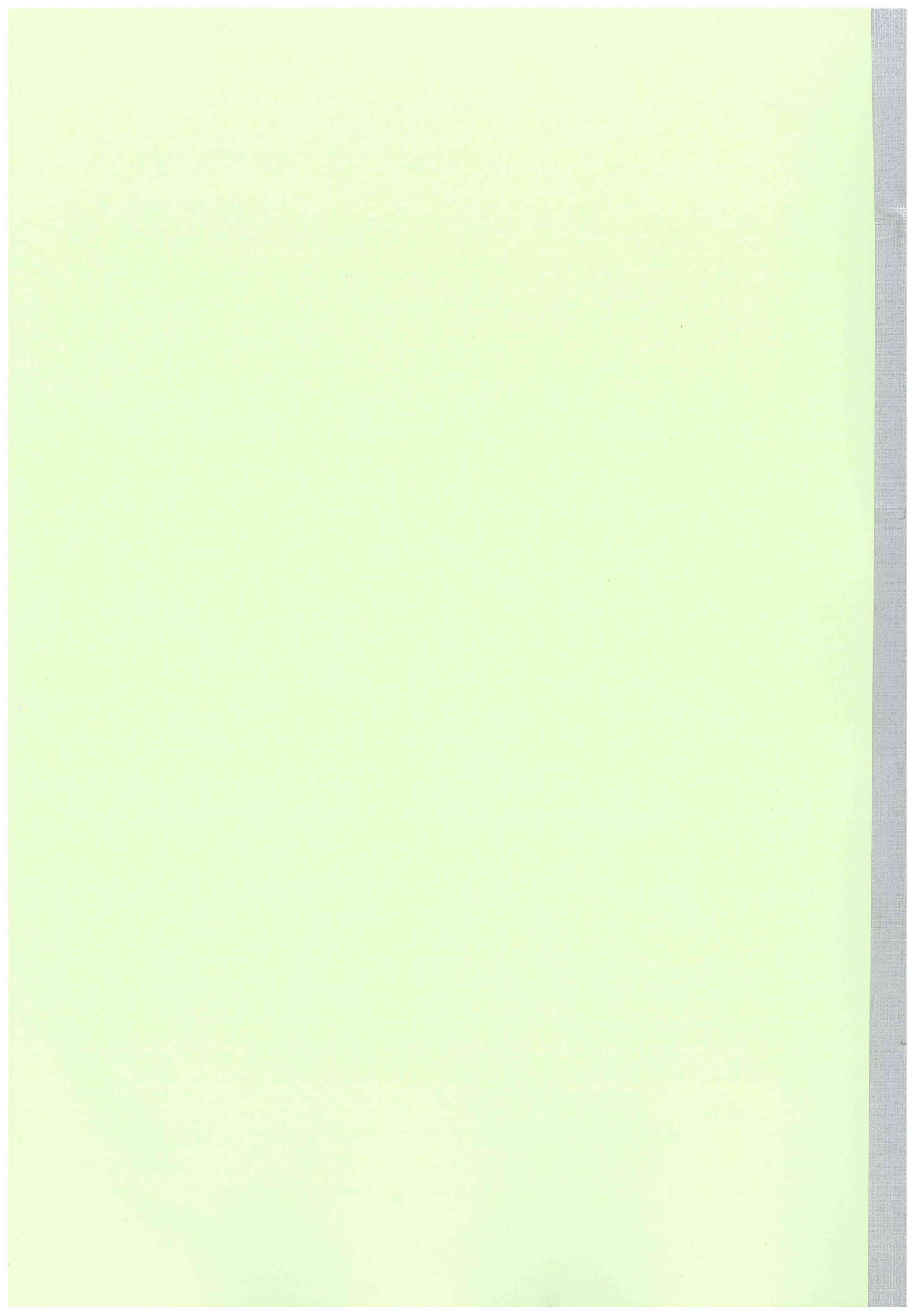
In conclusion, although the LVI detected by HE and EVG was a significant prognostic factor, the stage I lung adenocarcinoma patients who were determined to be LVI positive based on D2-40 immunostaining did not have a significantly poorer prognosis than the LVI negative cases. As we have previously reported, using HE and EVG staining may be sufficient to diagnose LVI, and it can thus be used as a significant prognostic factor for patients with adenocarcinoma of the lung. Future studies will be needed to investigate the correlation between D2-40 staining and the expression of either biomarkers or tumor markers.

ACKNOWLEDGMENT

This contribution was supported, in part, by the Grants-in-Aid for the U.S.-Japan Cooperative Medical Science Program; the National Cancer Center Research and Development Fund; Grant for priority areas from the Japanese Ministry of Education, Culture, Sports, Science and Technology [221S0001]; and Grants-in-Aid for Cancer Research from the Japanese Ministry of Health, Labour and Welfare [23120201 and 10103838], Smoking Research Foundation, and Princess Takamatsu Cancer Research Fund.

REFERENCES

- Parkin DM, Bray F, Ferlay J, Pisani P. Global cancer statistics, 2002. *CA Cancer J Clin* 2005; **55**: 74–108.
- Sawabata N, Asamura H, Goya T *et al*. Japanese Lung Cancer Registry Study: First prospective enrollment of a large number of surgical and nonsurgical cases in 2002. *J Thorac Oncol* 2010; **5**: 1369–75.
- Iwakoshi A, Murakumo Y, Kato T *et al*. RET finger protein expression is associated with prognosis in lung cancer with epidermal growth factor receptor mutations. *Pathol Int* 2012; **62**: 324–30.
- Goldstraw P. *Stageing Manual in Thoracic Oncology*. Denver: IASLC, 2009.
- Gabor S, Renner H, Popper H *et al*. Invasion of blood vessels significant prognostic factor in radically resected T1-3N0M0 non-small-cell lung cancer. *Eur J Cardiothorac Surg* 2004; **25**: 439–42.
- Urabe A, Matsumoto T, Kimura M, Sonoue H, Kinoshita K. Grading system of lymphatic invasion according to D2-40 immunostaining is useful for the prediction of nodal metastasis in squamous cell carcinoma of the uterine cervix. *Histopathology* 2006; **49**: 493–7.
- Walgenbach-Bruenagel G, Tolba RH, Varnai AD, Bollmann M, Hirner A, Walgenbach KJ. Detection of lymphatic invasion in early stage primary colorectal cancer with the monoclonal antibody D2-40. *Eur Surg Res* 2006; **38**: 438–44.
- Van den Eynden GG, Van der Auwera I, Van Laere SJ *et al*. Distinguishing blood and lymph vessel invasion in breast cancer: A prospective immunohistochemical study. *Br J Cancer* 2006; **94**: 1643–9.
- Yonemura Y, Endou Y, Tabachi K *et al*. Evaluation of lymphatic invasion in primary gastric cancer by a new monoclonal antibody, D2-40. *Hum Pathol* 2006; **37**: 1193–9.
- Kadota K, Huang CL, Liu D *et al*. The clinical significance of the tumor cell D2-40 immunoreactivity in non-small cell lung cancer. *Lung Cancer* 2010; **70**: 88–93.
- Min KH, Park SJ, Lee KS *et al*. Clinical usefulness of D2-40 in non-small cell lung cancer. *Lung* 2011; **189**: 57–63.
- Funai K, Sugimura H, Morita T, Shundo Y, Shimizu K, Shiya N. Lymphatic vessel invasion is a significant prognostic indicator in stage IA lung adenocarcinoma. *Ann Surg Oncol* 2011; **18**: 2968–72.
- Travis WD, Brambilla E, Muller-Hermelink H, Harris CC. *Pathology and Genetics of Tumours of the Lung, Pleura, Thymus and Heart*. Lyon: IARC Press, 2004.
- Travis WD, Brambilla E, Noguchi M *et al*. International Association for the Study of Lung Cancer/American Thoracic Society/European Respiratory Society International multidisciplinary classification of lung adenocarcinoma. *J Thorac Oncol* 2011; **6**: 244–85.
- Igarashi H, Sugimura H, Maruyama K *et al*. Alteration of immunoreactivity by hydrated autoclaving, microwave treatment, and simple heating of paraffin-embedded tissue sections. *APMIS* 1994; **102**: 295–307.
- Bréchet JM, Chevret S, Charpentier MC *et al*. Blood vessel and lymphatic vessel invasion in resected nonsmall cell lung carcinoma. Correlation with TNM stage and disease free and overall survival. *Cancer* 1996; **78**: 2111–18.
- Kahn HJ, Marks A. A new monoclonal antibody, D2-40, for detection of lymphatic invasion in primary tumors. *Lab Invest* 2002; **82**: 1255–7.
- Iwakiri S, Nagai S, Katakura H *et al*. D2-40-positive lymphatic vessel density is a poor prognostic factor in squamous cell carcinoma of the lung. *Ann Surg Oncol* 2009; **16**: 1678–85.
- Faoro L, Hutto JY, Salgia R *et al*. Lymphatic vessel density is not associated with lymph node metastasis in non-small cell lung carcinoma. *Arch Pathol Lab Med* 2008; **132**: 1882–8.
- Inoue M, Takakuwa T, Minami M *et al*. Clinicopathologic factors influencing postoperative prognosis in patients with small-sized adenocarcinoma of the lung. *J Thorac Cardiovasc Surg* 2008; **135**: 830–36.
- Hashizume S, Nagayasu T, Hayashi T *et al*. Accuracy and prognostic impact of a vessel invasion grading system for stage IA non-small cell lung cancer. *Lung Cancer* 2009; **65**: 363–70.



201313013B (2/2)

厚生労働科学研究費補助金
第3次対がん総合戦略研究事業

ゲノム・遺伝子解析に基づく、胃がん、肺腺がん高危険度群の
捕捉、及び予防標的分子の同定に資する研究

平成22～25年度 総合研究報告書
(II)

研究代表者 梶村 春彦

平成26年5月

Accumulated phosphatidylcholine (16:0/16:1) in human colorectal cancer; possible involvement of LPCAT4

Nobuya Kurabe,¹ Takahiro Hayasaka,² Mikako Ogawa,³ Noritaka Masaki,² Yoshimi Ide,^{2,3} Michihiko Waki,² Toshio Nakamura,⁴ Kiyotaka Kurachi,⁴ Tomoaki Kahyo,¹ Kazuya Shinmura,¹ Yutaka Midorikawa,⁵ Yasuyuki Sugiyama,^{6,7} Mitsutoshi Setou^{2,8} and Haruhiko Sugimura^{1,8}

Departments of ¹Tumor Pathology; ²Cell Biology and Anatomy; ³Surgery I (Breast Surgery); ⁴Surgery II (Colorectal Surgery), Hamamatsu University School of Medicine, Shizuoka; ⁵Department of Digestive Surgery, Nihon University School of Medicine, Tokyo; ⁶Department of Surgery, Gifu Municipal Hospital, Gifu; ⁷Department of Surgery, Teikyo University School of Medicine University Hospital, Kawasaki, Japan

(Received December 4, 2012/Revised June 17, 2013/Accepted June 22, 2013/Accepted manuscript online July 2, 2013)

The identification of cancer biomarkers is critical for target-linked cancer therapy. The overall level of phosphatidylcholine (PC) is elevated in colorectal cancer (CRC). To investigate which species of PC is overexpressed in colorectal cancer, an imaging mass spectrometry was performed using a panel of non-neoplastic mucosal and CRC tissues. In the present study, we identified a novel biomarker, PC(16:0/16:1), in CRC using imaging mass spectrometry. Specifically, elevated levels of PC(16:0/16:1) expression were observed in the more advanced stage of CRC. Our data further showed that PC(16:0/16:1) was specifically localized in the cancer region when examined using imaging mass spectrometry. Notably, because the ratio of PC(16:0/16:1) to lyso-PC(16:0) was higher in CRC, we postulated that lyso-PC acyltransferase (LPCAT) activity is elevated in CRC. In an *in vitro* analysis, we showed that LPCAT4 is involved in the deregulation of PC(16:0/16:1) in CRC. In an immunohistochemical analysis, LPCAT4 was shown to be overexpressed in CRC. These data indicate the potential usefulness of PC(16:0/16:1) for the clinical diagnosis of CRC and implicate LPCAT4 in the elevated expression of PC(16:0/16:1) in CRC. (*Cancer Sci*, doi: 10.1111/cas.12221, 2013)

Colorectal cancer (CRC) is the fourth most common cancer worldwide and causes approximately 600 000 deaths per year.⁽¹⁾ Previous studies have reported that CRC contains increased amounts of phospholipids as well as an altered phospholipid composition of the CRC cell membrane.^(2,3) These changes in membrane phospholipid levels can affect cell proliferation, viability and tumor development.^(2,4) Moreover, although phosphatidylcholine (PC) is the most dominant phospholipid in both non-neoplastic and cancer tissues,⁽⁵⁾ the amount of PC is highly increased in CRC cells.⁽²⁾ In addition, the changes in membrane potential and the increased PC/phosphatidylethanolamine (PE) composition rate are related to the grade of CRC malignancy.⁽³⁾ In higher eukaryotes, PC is synthesized via two pathways: (i) the triple methylation of PE; and (ii) the cytidine diphosphate (CDP)-choline pathway.⁽⁶⁾ However, the steady-state composition of PC species is maintained by the remodeling cycle (Lands' cycle).⁽⁷⁾ The precise and concerted deacylation by phospholipase A₂ (PLA₂) and reacylation by lyso-PC acyltransferase (LPCAT) are required for normal cell functioning. Notably, the elevated expression of LPCAT1 was associated with colon cancer growth.⁽⁸⁾ LPCAT1 is a member of the LPCAT family (LPCAT1-4) and shows LPCAT activity, preferentially incorporating palmitate into PC.⁽⁸⁾ However, the relationship between PC remodeling and the progression of cancer, as well as the class of LPCAT involved in this process, remains unclear.

Direct mass spectrometry (MS) of biological tissue sections using matrix-assisted laser desorption/ionization (MALDI) can profile many molecules including phospholipid subtypes.⁽⁹⁾ Furthermore, this approach can be extended to imaging MS, which can visualize the distribution of biomolecules in the tissue section.⁽¹⁰⁻¹³⁾ Because specific antibodies against lipids and macromolecules are often difficult to obtain, MALDI imaging is a suitable option for detecting distinct species of these molecules directly in a tissue section. This technique has already been applied to various human cancers including prostate and gastric cancer.^(14,15) Although this emerging analytical technique was initially developed as a tool for protein imaging, recently it has been increasingly used for the imaging of small organic molecules including lipids.⁽¹⁶⁾ We have developed an innovative instrument that we called a mass microscope.⁽¹⁷⁾ A mass microscope enables the molecules in a tissue sample to be ionized while preserving positional information regarding where the molecules have been ionized using 2-D laser scanning. The ionized molecules are analyzed using a time-of-flight (TOF)-type mass spectrometer and are presented as multiple biomolecules according to their mass-to-charge ratio (*m/z*). The distribution of the biomolecules is then visualized in 2-D as the signal intensity among the measurement points on the image of the tissue section.

In the present study, we applied mass microscopy to human CRC tissues as a non-targeted screening for PC biomarkers to obtain a novel molecular profile. We then performed a principal component analysis (PCA) of the data and successfully identified a difference between CRC cells and adjacent non-neoplastic colorectal mucosal cells. One PC(16:0/16:1) was visualized as differentially expressed molecules between the CRC and non-neoplastic mucosa areas. Because this PC species is known to be associated with metabolism by LPCAT families, we further specified which LPCAT (LPCAT1-4) contributes to the increase in PC(16:0/16:1) in CRC.

Materials and Methods

Tissue/clinicopathological data. All samples were retrieved from the archive of Hamamatsu University Hospital. Tissue slides were evaluated histologically and graded according to the WHO classification. Cancer and corresponding non-neoplastic mucosa samples obtained from colorectal surgical specimens were snap-frozen in liquid nitrogen and stored at -80°C until required. Table 1 summarizes the clinicopathological

⁸To whom correspondence should be addressed.
E-mails: hsugimur@hama-med.ac.jp; setou@hama-med.ac.jp

profiles of the samples. The study protocol was approved by the institutional review board of Hamamatsu University School of Medicine.

Sample preparation. Sample preparation was done according to the previous literature⁽¹⁸⁾ and the details are in the Supporting Information.

Imaging MS analysis. All imaging MS analyses were performed using an atmospheric pressure-MALDI with a quadrupole ion trap-TOF analyser instrument, the mass microscope equipped with a diode-pumped 355 nm Nd:YAG laser (Shimadzu, Kyoto,

Japan).⁽¹⁷⁾ All the mass spectra were acquired using Mass Microscope System software (Shimadzu). This software consists of a graphical user interface that allows the user to specify the area to be imaged, the distance between laser shots (spatial resolution), the instrument acquisition method to be used, the number of laser shots to be irradiated at each spot and the mass range of interest to monitor. The sample was irradiated using a focused laser beam in synchrony with the stage scanning. A mass spectrum was acquired for each spot on the tissue surface. Ion images showing the localization of compounds within the sample were then obtained. The mass microscope measurements were performed in the reflection mode within a mass range of m/z 500–1200 using a scan pitch with a pixel size of 7.5 μm . The laser shot number and frequency were 200 per pixel and 1000 Hz, respectively. Following the imaging MS analysis, the matrix was washed with 70% ethanol and the sections were stained with H&E and photographed using a Keyence BZ-9000 (Keyence, Tokyo, Japan). The H&E-stained sections were co-registered with the imaging MS results and evaluated histologically by an experienced surgical pathologist. The lipid peak assignments were made by comparing each peak's mass measurement with the LIPID MAPS database (<http://lipidmaps.org>) and confirmed using MS/MS analyses (QSTAR Elite; Applied Biosystems, Foster City, CA, USA). Image reconstruction was performed using the software BioMap (freeware; www.maldi-msi.org).⁽¹⁹⁾

Data analysis and statistical analysis. Using ClinProTools 2.2 (Bruker Daltonics, Bremen, Germany), all spectra were subjected to baseline subtraction, smoothing, normalization to their own total ion current and recalibration. For each spectrum the total ion count was determined using the sum of all intensities of the spectrum. The spectra processing parameters were: baseline correction (Top Hat algorithm, minimal baseline width set to 10%); resolution (500 ppm); and smoothing (Savitzky Golay, five cycles with 2 m/z width). All spectra were recalibrated to reduce mass shifts. Peak picking was also per-

Table 1. Patient characteristics

Sex	
Male	24
Female	10
Age (years)	
<60	11
≥60	23
Mean ± SD	65.4 ± 13.1
Location	
Ascending colon	2
Transverse colon	4
Descending colon	1
Sigmoid colon	13
Rectum	14
Stage	
I	4
II	17
III	10
IV	3
Histopathological grading	
Well differentiated	20
Moderately differentiated	12
Poorly differentiated	2

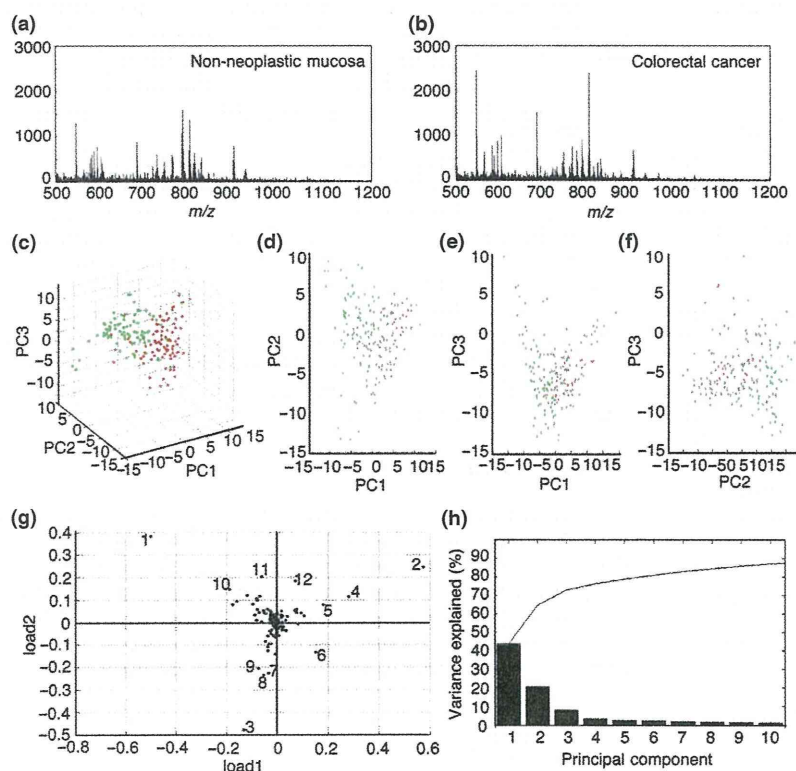


Fig. 1. Principal component analysis (PCA) of non-neoplastic mucosa and colorectal cancer (CRC). Representative mass spectra from (a) non-neoplastic mucosa and (b) CRC. (c) 3-D plotting graph of PCA. Red, CRC; green, non-neoplastic mucosa. (d-f) Corresponding 2-D graph of plotted PCA. (g) Loading plot of principal component 1 and principal component 2. The numbered components (No. 1–12) are summarized in Table 2. (h) Variance plot of principal components.

Table 2. Summary of different mean peak intensities between non-cancerous mucosa and cancerous mucosa

No.†	<i>m/z</i>	Non-cancerous mucosa	Cancerous mucosa	<i>P</i> -value‡
1	798.5	68.6 ± 30.4	96.4 ± 30.1	0.0001
2	545.0	54.6 ± 20.5	34.7 ± 20.6	0.0011
3	782.5	52.1 ± 20.6	39.6 ± 21.5	0.0003
4	770.5	7.1 ± 3.2	22.5 ± 13.3	0.000001
5	546.0	20.1 ± 10.5	13.7 ± 10.6	0.0019
6	585.0	27.3 ± 10.7	14.5 ± 7.8	0.0001
7	725.5	24.1 ± 10.1	16.4 ± 10.7	0.0001
8	780.5	27.3 ± 10.8	15.9 ± 8.3	0.0001
9	783.5	23.9 ± 10.1	18.3 ± 9.6	0.0011
10	799.5	21.6 ± 9.7	33.1 ± 11.1	0.0001
11	754.5	5.7 ± 2.4	10.0 ± 3.1	0.0001
12	601.0	23.2 ± 9.1	26.7 ± 12.0	0.0707

m/z, mass-to-charge ratio. †Numbers in this column correspond to those depicted in Figure 1(g). ‡Welch's *t*-test.

formed based on the overall average spectrum over the whole mass range (signal to noise threshold of 5). Multivariate statistical analyses were performed using the supervised neural network algorithm. The pretreated data have been used for statistical analysis and visualization in ClinProTools and Bio-Map. There is no need for internal standards because it might interfere with the detection of isomeric endogenous lipids. The PCA was also performed using mean-centering and ClinProTools 2.2.^(20,21) The stage I colorectal cancer samples were not included in the PCA analysis because these samples might interfere with the separation of the PCA plots. The PCA results were represented using two multi-dimensional plots: a score plot and a loading plot. The score plot was based on the PCA and showed similarities and differences among the samples; samples with similar peak patterns were clustered closely within the plot. The loading plot showed the influence of the data variables (in this case, the *m/z* values). The score plot of the PCA results was presented as pseudo-color images. For all the intensity calculations for the non-neoplastic mucosa and CRC, the signal intensities were generated using the ClinProt Peak Statistic Calculation and the ratio of signal intensities was then calculated. Differences in the intensities or ratios between the non-neoplastic mucosa and CRC were assessed using Welch's *t*-test.

Cell culture, transfection and cell growth. HCT116 and DLD1 cells were obtained from the American Type Culture Collection (Rockville, MD, USA). The cells were cultured in RPMI1640 medium containing 10% fetal calf serum, as described previously.⁽²²⁾ Before cell culture, eight-well flexiPERM slide chambers (Sarstedt, Newton, NC, USA) were attached to the poly-L-lysine-coated indium tin oxide slide glass to form culture chambers. The cells (20 000 cells/well) were then seeded onto the culture chambers. Twenty-four hours after seeding, the cells were transfected with 40 nM siRNA targeted for LPCAT1, LPCAT2, LPCAT3, LPCAT4 and a negative control using Lipofectamine 2000 (Invitrogen, Carlsbad, CA, USA). Seventy-two hours after transfection, the cells were washed twice with water and then freeze dried. The dried cells were measured using a mass microscope as described in imaging MS analysis section. Each mass intensity value is the mean ± standard error (SE) of three independent experiments. For cell growth assay, HCT116 or DLD1 cells were transfected with siRNA targeted for LPCAT4 and then seeded in a 24-well plate. Cell counting was performed every day.

RNAi and quantitative PCR (qPCR). Details are provided in the Supporting Information. Stealth RNAi oligonucleotides were used for the siRNA experiment (Invitrogen).

LPCAT assay. Details of the LPCAT assay are in the Supporting Information. 50 µg of cell lysates were added to the reaction

buffer (80 mM Tris-HCl pH 7.4, 5 mM MgCl₂, 50 µM [¹⁴C] lysopalmitoyl phosphatidylcholine and 50 µM palmitoleoyl CoA; final volume 100 µL). The reaction was incubated at 24°C for 10 min and stopped by spotting 16 µL of the reaction onto a silica, thin-layer chromatography plate (Whatman, Maidstone, UK) together with lipid standard (PC[16:0/16:1]; Avanti Polar Lipids, Alabaster, AL, USA). The plates were developed in CHCl₃/acetic acid/methanol/water (60/30/10/4) and the incorporation of [¹⁴C] into PC was analyzed using a BIOSCAN AR-2000 (BIOSCAN, Washington, DC, USA). The standard was stained with iodine vapor.

Tissue microarray (TMA), immunohistochemistry and western blotting. Details on TMA construction and immunohistological evaluation are based on previous literature⁽²³⁾ and in the Supporting Information. Briefly, the expression of LPCAT4 in CRC was categorized according to the modified algorithm in previous literature, that is, the staining intensities were categorized as follows: blue (0); blue-brown (1); brown (2); and bright brown (3). The areas evaluated were a small core of the TMA (2 mm in diameter) and the apparent intratumor heterogeneity was negligible.^(24–26)

Western blotting was performed as described previously.⁽²²⁾ β-tubulin (1:1000) was used as an internal control. Anti-LPCAT4 antibody (1:1000) was also used as a primary antibody.

Results

Unsupervised analysis distinguishes CRC from non-neoplastic mucosa. For an in-depth comparison of cancer and non-neoplastic mucosa, sections from cancer and non-neoplastic mucosa were selected and the mass spectra acquired from those regions using the mass microscope were compared to identify specific cancer markers. Tissue sections with CRC or non-neoplastic mucosa from 30 patients (Table 1) were stained with H&E to distinguish among the non-neoplastic mucosa, stroma and cancerous areas. According to the H&E-stained tissue, two quadrat areas (one from the non-neoplastic mucosa area and the other from the cancerous area) were selected to obtain mass spectra using the mass microscope. Figure 1(a,b) shows the accumulated spectra from the non-neoplastic mucosa area and the cancerous area, respectively. Both mass spectra had a large number of signals in the mass range, corresponding to the phospholipids region (*m/z*, 700–850).⁽²⁷⁾

For the profiling experiments, spectra from each tissue were imported into the statistical analysis software ClinProTools^(20,21) and a PCA was performed. The first three principal components of the CRC and non-neoplastic mucosa profiling data revealed two specific groupings capable of characterizing CRC and the non-neoplastic mucosa (Fig. 1c). Principal components 1 and 2, which describe the largest variance in the data (Fig. 1h), distinguished CRC from non-neoplastic mucosa (Fig. 1d). The CRC and non-neoplastic mucosa showed a partial overlap for principal components 2 and 3 and for principal components 1 and 3 (Fig. 1e,f). The corresponding loading plot demonstrated the influence of the *m/z* value on the respective principal components (Fig. 1g). The signal intensity of these *m/z* values from CRC and the non-neoplastic mucosa are shown in Table 2 and are numbered in order of descending loading plot absolute values (No. 1–12). A Welch's *t*-test was performed on a data set comparing CRC and the non-neoplastic mucosa. To identify CRC biomarkers, we compared the intensity of these peaks. The mean peak intensity at *m/z* 770.5 in the CRC was three times higher than that of the non-neoplastic mucosa (Table 2). Thus, we considered that the peak at *m/z* 770.5 was a major candidate for a CRC biomarker.

Product ions assignment using MS/MS and its expression in CRC. On-tissue MS/MS was used to assign the peaks. The peak at *m/z* 770.5 was identified as that of PC based on the

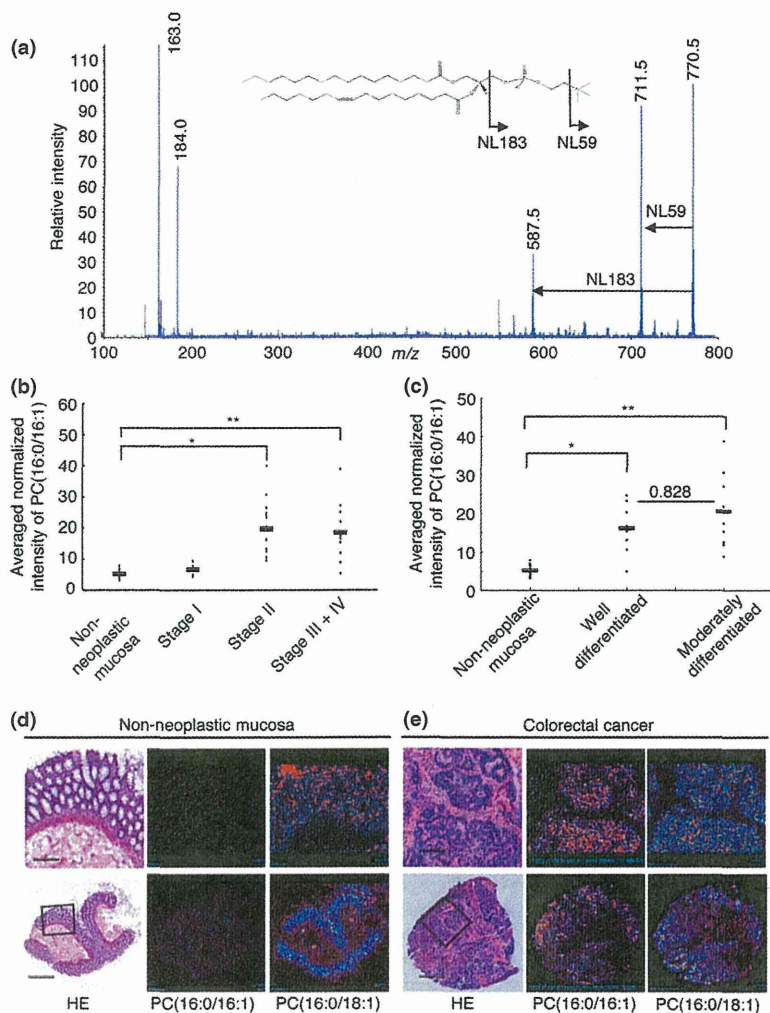


Fig. 2. The ion at the mass-to-charge ratio (m/z) of 770.5 can distinguish the non-neoplastic mucosa from colorectal cancer (CRC). (a) Direct MS/MS spectrum of the ion at m/z 770.5. The ions of the diagnostic fragments suggest that the ion at m/z 770.5 is that of PC(16:0/16:1). (b) Averaged normalized intensity values for PC(16:0/16:1) were plotted according to the pathological stage of CRC. The samples were analyzed using the mass microscope. The horizontal line indicates the median. $*P = 0.0027$. $**P = 0.0072$. (c) Normalized average intensity values for PC(16:0/16:1) were plotted according to the pathological differentiation state of CRC. The horizontal line indicates the median. $*P = 0.0028$. $**P = 9.3E-5$. (d, e) H&E-stained images (left) of non-neoplastic mucosa and CRC tissue and ion images showing spatial distribution of PC(16:0/16:1) (middle) and PC(16:0/18:1) (right). Bar, 150 μm (top); 600 μm (bottom). (d) 600 μm (top), 150 μm (bottom); (e) $\times 40$ (top), $\times 2.5$ (bottom). MS, mass spectrometry; NL, neutral loss; PC, phosphatidylcholine.

presence of fragment ions at an m/z value of 184 and a neutral loss of 59 and 183 in an MS/MS analysis, which is indicative of PC (Fig. 2a).^(28,29) LIPID MAPS suggested that these peaks at m/z 770.5 can be assigned as $(\text{PC}[16:0/16:1]+\text{K})^+$. Generally, PC is detected as $[\text{M}+\text{Na}]^+$ or $[\text{M}+\text{K}]^+$ ions in tissue sections; thus, the peak intensity at m/z 754.5 ($[\text{PC}(16:0/16:1)+\text{Na}]^+$) was compared between CRC and the non-neoplastic mucosa. We confirmed that the peak in CRC samples at m/z 754.5 was increased by 70% compared with those from the non-neoplastic mucosa (Table 2). In a subsequently examined section, $[\text{M}+\text{K}]^+$ ions were used to determine the intensities. To investigate the trend in PC(16:0/16:1) expression according to increasing disease stage and differentiation state of CRC, we examined the intensity of PC(16:0/16:1) in the sections. As shown in Figure 2(b,c), a significant trend toward an increased expression was observed in advanced-stage disease and every histological grade of CRC. Therefore, these results imply that PC(16:0/16:1) is a CRC-specific biomarker.

Visualization of ion images in CRC and non-neoplastic mucosa using a mass microscope. Colorectal cancer is comprised of a number of cell types, including cancerous and non-cancerous epithelial cells, non-epithelial stromal cells and infiltrating blood cells; therefore, an imaging modality such as the mass microscope is uniquely powerful for determining which areas actually contain PC(16:0/16:1). The left panel of Figure 2(d,e) shows a typical H&E stain of a thin section of non-neoplastic mucosa and CRC tissue showing regions of moderately differentiated adenocarcinoma with stromal tissues. The method

allowed a parallel assessment of the histopathological features seen under a light microscope and the phospholipid profiles obtained using the mass microscope (middle and right panel of Fig. 2d,e). A comparison of the PC(16:0/16:1) signatures obtained from CRC and the non-cancerous mucosa is also shown in the middle panel of Figure 2(d,e), clearly demonstrating a cancer-specific PC(16:0/16:1) distribution. In contrast, PC(16:0/18:1) (m/z 782.5, $[\text{PC}(16:0/18:1)+\text{Na}]^+$) was detected in both CRC cells and non-cancerous cells (right panel of Fig. 2d,e). Therefore, use of the mass microscope enabled the imaging of a CRC biomarker *in situ*.

Involvement of LPCAT4 in the synthesis of PC(16:0/16:1). To investigate the molecular mechanism responsible for the increase in PC(16:0/16:1), we calculated the ratio of PC(16:0/16:1) to lyso-PC(16:0) (m/z 518.3, $[\text{lyso-PC}(16:0)+\text{Na}]^+$) in CRC and the non-neoplastic mucosa. A higher ratio of PC(16:0/16:1)/lyso-PC(16:0) was observed in CRC (Fig. 3a). This result supports the hypothesis that the conversion of lyso-PC(16:0) into PC(16:0/16:1) is activated in CRC. Recently, LPCAT (LPCAT1-4) have been described as a novel enzyme family that catalyze lyso-PC into PC⁽³⁰⁻³⁴⁾ and exhibit substrate specificity for some kinds of fatty acid. If the increase in LPCAT activity in CRC is one reason for the increase in PC, the conversion of lyso-PC into PC through the catalysis of LPCAT should be elevated.⁽⁷⁾ To examine which member of LPCAT is involved in the deregulated level of PC(16:0/16:1) *in vitro*,

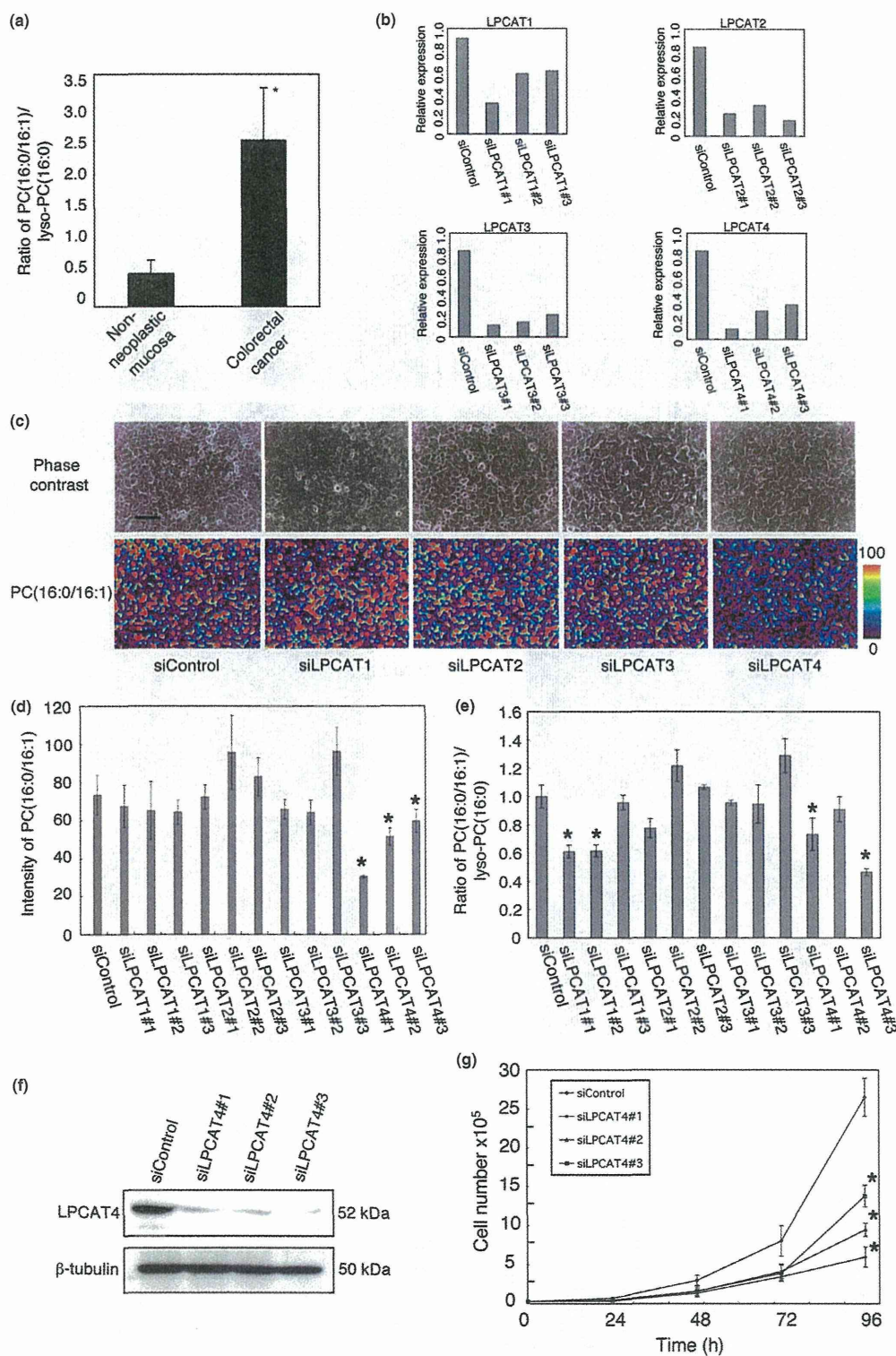


Fig. 3. Involvement of LPCAT4 in the synthesis of phosphatidylcholine (PC)(16:0/16:1) in colorectal cancer (CRC) *in vitro*. (a) The ratio of PC(16:0/16:1) to lyso-PC(16:0) was plotted for non-neoplastic mucosa and CRC. * $P = 5.1E-10$. (b) Efficiency of mRNA downregulation by siRNA targeted for LPCAT. The siRNA targeted for LPCAT or control siRNA were transfected into HCT116 cells. Forty-eight hours after transfection, total RNA were extracted and reverse transcription was performed. The LPCAT expression levels were quantitated using quantitative PCR. (c) Representative image of PC(16:0/16:1) in HCT116 cells analyzed using the mass microscope. Phase contrast images (top) and averaged normalized intensity images (bottom). Bar, 70 μm . (d) Effect of the downregulation of LPCAT on the averaged normalized intensity of PC(16:0/16:1). The siRNA targeted for LPCAT or control siRNA were transfected into HCT116 cells. Seventy-two hours after transfection, the cells were washed with water and then analyzed using the mass microscope. * $P < 0.05$. (e) LPCAT enzyme activities were analyzed using a LPCAT assay. The ratio of PC(16:0/16:1) to lyso-PC(16:0) was plotted for control and LPCAT siRNA. * $P < 0.05$. (f) Downregulation of LPCAT4 expression analyzed using western blotting. (g) Effect of LPCAT4 downregulation on cell growth. * $P < 0.05$. LPCAT, lyso-PC acyltransferase.